Phase effect in stopping of H ions in Mg

M. Bergsmann,[1] W. Raab,[1] G. Schrenk,[1] F. Kastner,[1] R. Díez Muiño,[2,3] A. Arnau,[3] A. Salin,[2] P. Bauer,[1,*] and P. M. Echenique[3]

[1]*Institut für Experimentalphysik, Johannes-Kepler-Universität Linz, Altenbergerstraße 69, A-4040 Linz, Austria*

[2]*Laboratoire de Physico-Chimie Moléculaire, UMR 5803 CNRS-Université de Bordeaux I, 351 Cours de la Libération, 33405 Talence Cedex, France*

[3]*Departamento de Física de Materiales, Universidad del País Vasco, Apartado 1072, San Sebastián, Spain*

(Received 4 February 2000)

We present measurements and calculations of electronic stopping of protons and deuterons in Mg (gas and solid) in the range 15–650 keV/A. The measurements were performed by transmitting the ion beam through a vapor cell containing solid and gaseous Mg in thermal equilibrium. In order to get absolute values of the stopping cross section ε, the experimental gas data were normalized by the requirement that the experimental phase effect $\Delta\varepsilon \equiv \varepsilon_{\mathrm{gas}} - \varepsilon_{\mathrm{solid}}$ —with the ε for metallic Mg from Bergsmann (1998)— is equal to the theoretical value $\Delta\varepsilon_{\mathrm{th}}$ at a reference energy of 400 keV. We have used a Hartree-Fock-Slater description of the Mg atom and the first Born approximation to calculate excitation and ionization of Mg in the gas phase and the ionization of the inner shells of solid Mg, while the valence electrons ($3s$) of solid Mg are described by a free-electron gas. Charge-exchange processes are explicitly taken into account to estimate both the equilibrium charge state fractions and the energy loss in charge-exchange processes, as required by our charge state approach. We obtain a pronounced phase effect of up to 70% at 20 keV. Theory and experiment coincide within the experimental uncertainties in a wide energy range; systematic deviations occur only at low energies where the linear model breaks down.

INTRODUCTION

In studies of the interaction of ions with matter,[1] the electronic stopping is an almost omnipresent quantity. It is common to characterize the energy loss in a collision of an ion (atomic number Z_1) with a target atom (atomic number Z_2) by the stopping cross section ε that is defined as the sum over all possible energy transfers T weighted by the corresponding cross section $d\sigma$,

$$\varepsilon = \int T d\sigma. \tag{1}$$

Equation (1) includes target excitation and ionization, projectile excitation, and charge exchange of the projectile (electron capture and loss).

In the gas phase, the ion-target interaction is due to the interatomic potential that depends strongly on the atomic charges Z_1 and Z_2 of the collision partners and on the states of the electrons bound to the projectile. In a metal, however, the interaction is strongly influenced by the screening of the intruder charge by the conduction electrons.[2] Even in large band-gap insulators, the band structure has been found to be so strongly perturbed by the ion that the band gap has no influence on the electronic stopping at low ion velocities.[3] The intrinsic difference between the ion-atom interaction in the solid and in the gas phase leads, for a given ion, to a dependence of the stopping cross section on the state of aggregation of the material.

As a quantitative measure for the gas-solid phase effect, we define the difference $\Delta\varepsilon = \varepsilon_{\mathrm{gas}} - \varepsilon_{\mathrm{solid}}$, where the suffixes refer to the specific states of aggregation. We stress that the pure phase effect can only be investigated in the case of a target that contains just one chemical element, since for any compound it is much more difficult to separate the phase effect clearly from chemical state effects that appear as a consequence of the chemical bonds.

In a previous study we have investigated the phase effect for H ions in Zn,[4,5] and found a rather pronounced gas-solid difference of up to 50%. The magnitude of the phase effect was explained theoretically by taking into account the various charge states of the projectile, the various valence electron states, and the screening of the projectile field in the solid.

The electronic structure of Zn is rather complex ($[\mathrm{Ar}]3d^{10}4s^2$), and at the stopping-power maximum at least 12 electrons contribute effectively to the deceleration process. In the present study, we investigate the phase effect for an electronically less complex system like an alkali or an alkali-earth element. Na has one valence electron with an ionization energy of 5.1 eV, while Mg has two valence electrons and a somewhat higher ionization energy (7.6 eV). We decided to use Mg as a target, because it is much less reactive than Na. As compared to the heavier alkali-earth metals, Mg has the advantage of having less multiple scattering resulting in a rather high transmitted intensity at low ion energies. As compared to Zn, for Mg a larger phase effect is expected for Mg due to its lower excitation energy. As projectiles we selected H ions.

EXPERIMENT

A mass and energy selected beam of H ions (protons or deuterons) in the energy range 40–700 keV is obtained from the Van de Graaff accelerator AN 700 at the University of Linz. The energy loss measurements have been performed using the setup ACOLITA (Apparatus for Collisions of Light

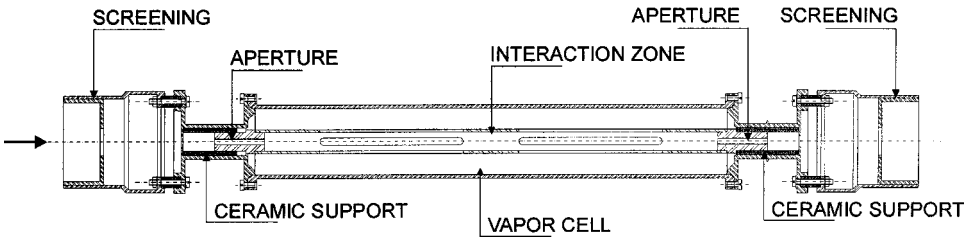

FIG. 1. Design of the vapor cell used in the experiment.

Ions with Target Atoms) which is a UHV system that permits energy-loss investigations in gaseous and solid targets.[6–8] Part of this setup is a vacuum chamber, which contains all the equipment needed for the production of the metal vapor. Special emphasis was put on protection of the apertures of the vapor cell and of the parts surrounding the cell against deposition of the vapor (see Figs. 1 and 2).

The vapor cell is made of stainless steel and is of cylindrical shape with an inner diameter of about 40 mm and a length of approximately 300 mm. In order to separate the ion-vapor interaction zone from the reservoir of metal, the vapor cell contains an inner cylinder with a diameter of 10 mm, and large openings towards the vapor cell for the vapor atoms to enter and leave the interaction zone. At its ends, the interaction tube has apertures to let the ion beam pass through the cell. The apertures have a diameter of 3 mm and a length of 30 mm. Since the ion beam has a diameter of about 1.5 mm, the adjustment of the vapor cell with respect to the beam is easier and the effusion of Mg vapor is reduced more efficiently, than with a thin aperture of the same diameter as the beam. The interaction tube is thermally isolated from the vapor cell by ceramic supports. Thus it stays at somewhat higher temperatures than the cell, when cooling the system. In thermal equilibrium it has the same temperature as the vapor cell. This design efficiently prevents the condensation of metal vapor in the region of the apertures (see Fig. 1).

The vapor cell is indirectly heated by a cylindrical oven made of copper and heated by commercial heating elements (Türk-Hillinger, HLP 120019). This design has the advantage of a rather homogeneous heating of the cell, but unfortunately the heating elements turned out to be suitable for UHV only to a limited extent. The vapor cell can be aligned *in situ* with respect to the ion beam, by means of linear motion feedthroughs attached to a pair of *xy* manipulators carrying the ends of the vapor cell (the *z* axis being the beam direction).

The temperature of the vapor cell is measured using three mantled thermocouples, mounted at the entrance, the center and the exit position on the outside of the vapor cell. The density of the vapor is obtained from the thermocouple readings using the vapor pressure curve[9] and the ideal gas equation. The temperature of the vapor cell is kept constant by means of a computer control[7,10] to within ± 0.2 degrees. The range of areal densities used for the energy-loss measurements (typically 10^{16}–10^{17} atoms/cm^2) corresponds to temperatures of 490–575 °C, well below the melting point at 650 °C. The first step after outgassing of the material was to heat the vapor cell to temperatures well above the melting point, in order to have reproducible conditions, i.e., a homogeneous Mg distribution on the inner surface of the vapor cell, and to avoid an unknown vapor pressure due to oxide layers at the surface of the Mg metal granules in the reservoir. The energy-loss experiments were then performed using the vapor in thermal equilibrium with the solid Mg surface.

We note that due to the high vapor pressure at 650 °C (about 10 mbars) effusion out of the vapor cell and condensation of the vapor at its colder parts, like the apertures, are nontrivial problems, which were overcome by use of the interaction tube (see above). Due to the high temperatures, the large amount of hot Mg involved in this experiment and the long heating cycles (typically a couple of days in a run) we run the vacuum system under computer control. A process computer reads all the relevant input data like pressure, temperature, status of valves, etc. In case of any disturbance the heating of the vapor cell would have been terminated and the cooling of the oven by dry N_2 gas be activated without breaking the vacuum.

The energy-loss measurements were performed in the following way: at a constant vapor density the ions at all required primary energies were transmitted through the vapor and their energy was measured after backscattering from a thin Pt marker (on carbon) by means of a Si detector (PIPS). This procedure requires a very precise and reproducible setting of the primary energy of the ion beam, with an uncertainty that is small compared to the energy loss measured, which is of the order of 1 keV. In a systematic study we investigated how reproducible the energy setting of our accelerator is within one day, and found it better than 50 eV at low energies. At high energies, the relative uncertainty is better than 10^{-4}, if done properly. This is sufficient for our purpose. We estimate that 200 eV (including primary energy and peak evaluation) is a conservative guess for the uncertainty in our energy-loss measurements. The reproducibility of setting the vapor temperature is believed to be of the order of ± 0.2 K. The absolute value of the vapor pressure is lim-

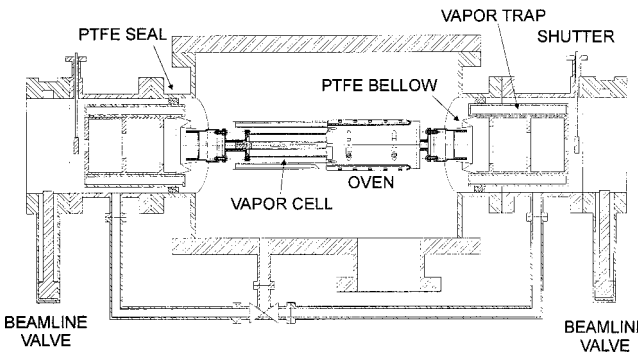

FIG. 2. Vacuum system containing the vapor cell and the condensation traps.

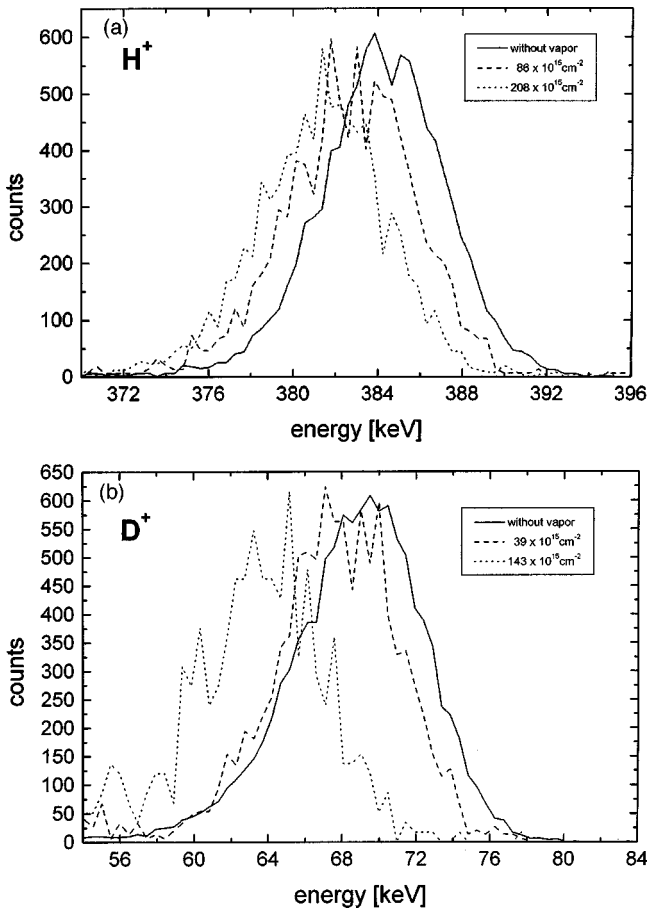

FIG. 3. RBS spectra of the Pt marker for (a) 390-keV protons and (b) 70-keV deuterons without Mg vapor and for various areal vapor densities (see inserts).

ited by the calibration of the temperature reading and the accuracy of the vapor pressure curve, which altogether leads to an uncertainty of about 20% for the Mg areal density.

In Fig. 3 we show the Rutherford-backscattering spectroscopy (RBS) spectra for 70-keV deuterons and for 390-keV protons for various areal densities nL of the Mg vapor (n denotes the Mg density and L the length of the vapor cell). The mean positions of the peaks yield the energy loss $\Delta E(nL)$. Absolute stopping cross-section data are then obtained as the ratio of the energy loss and the vapor density, $\Delta E/nL$. In our case, the uncertainty of the vapor density (20%) is too large to permit absolute measurements of sufficient accuracy. Therefore we determine the stopping cross-section values from the slopes of the linear fits to the ΔE data versus nL for each primary energy (see Fig. 4). In doing so, we make use of the high precision of the thermocouple reading. In this way, we obtain the energy dependence of the stopping cross section with a precision of typically 7% and fix the absolute value such that the measured phase effect equals the calculated one at the reference energy. As a reference we have chosen the stopping cross section (SCS) of 400-keV protons as shown in Fig. 4(a) as a compromise between sufficiently high energy to make the theoretical values reliable, and sufficiently low energy to have good experimental accuracy. Figure 4 further shows the $\Delta E(nL)$ data for 70-keV D^+ projectiles. This data set is again well fitted by a straight line. The fact that the fit intersects the abscissa

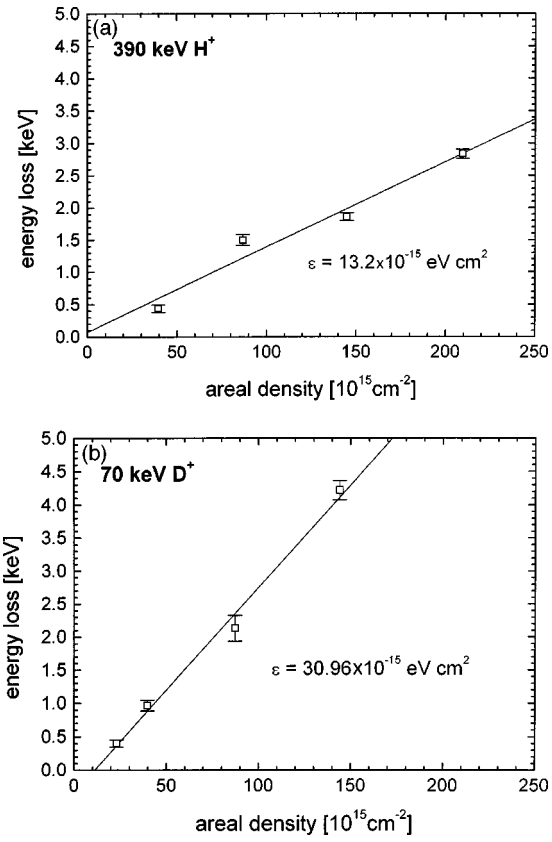

FIG. 4. Energy loss of (a) 390-keV protons and (b) 70-keV deuterons are shown as a function of the areal density of the Mg vapor. The stopping cross section is obtained from the slope of the linear fit to the experimental data.

at positve values indicates a reduced energy loss at very low densities, due to impact parameter selection in that regime.[11] We stress the point that our procedure to evaluate the stopping cross section from the slope of the $\Delta E(nL)$ data is not affected by impact parameter selection, which only occurs at densities much lower than those used in the present experiment.

Our experimental results for the stopping cross section of Mg vapor for H ions are shown in Fig. 5: The stopping maximum has a height of about $31\times10^{-15}\,\mathrm{eV\,cm^2}$, which is

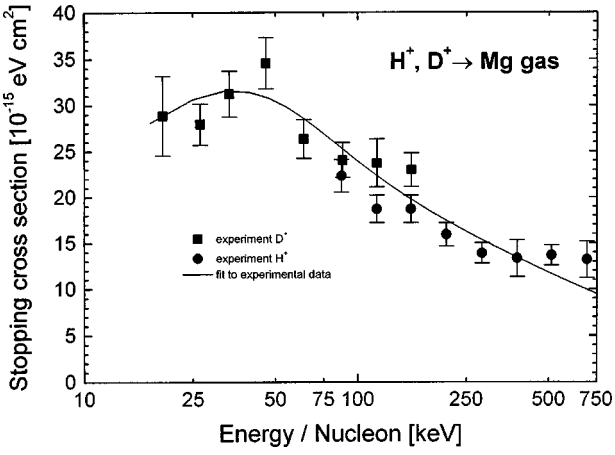

FIG. 5. Experimental results for the stopping cross section of H^+ (circles) and D^+ (squares) ions in Mg vapor.

quite different from the characteristics of the stopping maximum of the solid Mg, where the height of the stopping maximum was found[8,12] to be 21×10^{-15} eV cm^2. Note that the deuteron data and the proton data are consistent in the overlapping energy range within the combined experimental errors, giving further confidence in the experimental procedure.

THEORY

A crucial point in our approach is an accurate description of the charge state distribution. The screening due to an electron bound to the projectile implies a large difference between the SCS of a proton and that of a neutral hydrogen projectile. The difference is even larger in the gas phase. Details of the theoretical model are given in Ref. 5 and only briefly summarized here.

The Mg atom has a simple electronic structure consisting of a Ne-like core plus two $3s$ electrons in the M shell. We describe the electrons of the Mg atom within the Hartree-Fock-Slater (HFS) approximation[13] and calculate their excitation and ionization by protons using first born approximation (FBA).[14] For the neutral hydrogen fraction we also account for the screening by the bound projectile electron.

In the solid phase the Mg outer shell ($3s$) electrons form a band that we describe by a free-electron-like model ($r_s=2.7$) including electron hole pair and plasmon excitations. The inner shell electron contribution to stopping is calculated in FBA for the HFS atom as if it were in the gas phase, but using the correct relative energy level position and neglecting the excitation channel, i.e., including only ionization.

For Mg gas, we calculated the equilibrium charge state distribution of protons using the experimentally measured capture (σ_c) and loss (σ_l) cross sections.[15–17] These cross sections were also used to estimate the SCS in charge exchange processes ($\varepsilon_{c,l}$) assuming mean values for the transition energy in capture (T_c) and loss (T_l) processes. The relative weight of the different Mg orbitals in the total capture cross section was evaluated with the help of the continuum distorted wave (CDW) approximation.[18] The expression of $\varepsilon_{c,l}$ is

$$\varepsilon_{c,1}=\sum_i \sigma_{c,1}^{(i)}\cdot T_{c,1}^{(i)}, \tag{2}$$

where the sum over i runs over all possible capture and loss channels and the mean transition energies considered are

$$T_c^{(i)}=\Delta E_b^{(i)}+\tfrac{1}{2}mv^2, \tag{3}$$

$$T_l=-E_{\rm H}+E_{\rm el}. \tag{4}$$

Here, $\Delta E_b^{(i)}=E_{\rm H}-E_{\rm Mg}^{(i)}$ is the difference between the binding energy of the hydrogen $1s$ orbital, $E_{\rm H}$, and the HFS binding energy of the Mg orbital i, $E_{\rm Mg}^{(i)}$. v is the projectile velocity, m the mass of the electron, and $E_{\rm el}$ is the mean energy of the electron in the continuum state.

For the solid phase, we calculated the capture and loss cross sections, as there are no experimental data available except those affected by surface effects.[19] The $3s$ electron capture by the moving proton as well as the loss process due to the interaction with valence electrons are described as a dynamic Auger process in the electron gas.[2] The Mg L shell electron capture by protons is calculated in the CDW approximation. Finally, the contribution of the Mg lattice of Mg^{2+} ion cores to the loss cross section has been estimated by scaling the Al data from Ref. 2.

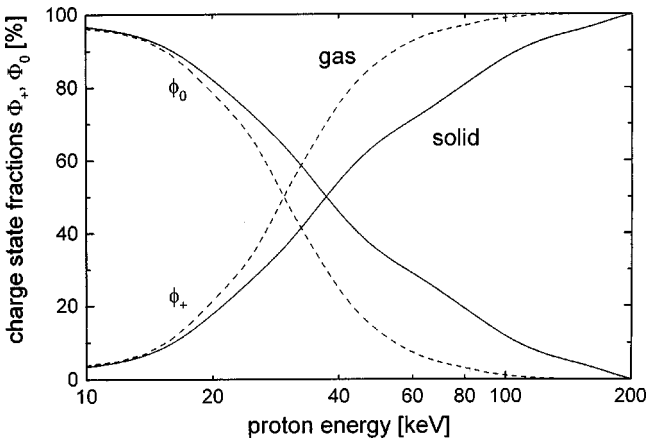

FIG. 6. Equilibrium charge state fractions for protons (Φ_+) and for neutral hydrogen (Φ_0) for the solid and the gas phase of Mg.

The total stopping cross section ε is obtained as a sum of partial SCS, ε_i, weighted by the corresponding charge state fractions Φ_i plus the contribution of capture and loss processes ($\varepsilon_{c,l}$):

$$\varepsilon=\sum_i \Phi_i[\varepsilon_i+\varepsilon_{i;c,l}]. \tag{5}$$

RESULTS AND DISCUSSION

In Fig. 6 we plot the equilibrium charge state fractions of protons and neutral hydrogen atoms traveling inside gas and solid Mg targets, as a function of projectile energy. Over the entire energy range the mean charge state of the projectile is lower in the solid phase. This is primarily due to the restriction in the number of unoccupied available states in the electron-loss process when the target is the solid, where the $3s$ electrons form an extended valence band. As a consequence the value of the electron-loss cross section is lower in the solid than in the gas phase. The capture cross section does not differ too much between the two phases. The transition from a pure proton beam (at high energies) to a beam predominantly composed of neutral hydrogen projectiles (at low energies) is slower in the solid phase.

We plot in Fig. 7 the theoretical SCS for hydrogen projectiles in Mg gas as a function of the projectile energy. We also represent in Fig. 7 the contributions to the SCS from each charge state and from the capture and loss of electrons by the projectile. The shape of the total SCS is mainly determined by the SCS of the proton fraction. It presents a maximum value of $\varepsilon=32.1\times10^{-15}$ eV cm^2 at a projectile energy of 40 keV. At energies below 100 keV the main contribution to the SCS is the $3s\rightarrow3p$ excitation of the Mg atom. It amounts to roughly 80% of the total SCS at 100 keV. The $3s\rightarrow3p$ excitation is a dipolar transition with a low transition energy (3.3 eV in our HFS calculation) and a large cross section. When the projectile energy decreases and the predominant charge state is neutral hydrogen, the capture

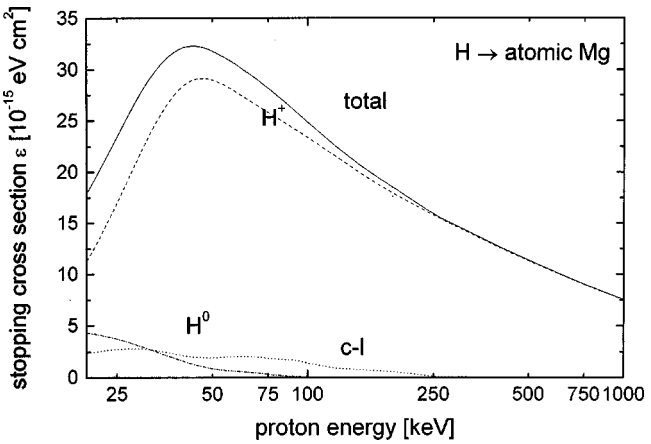

FIG. 7. Theoretical stopping cross section ε for hydrogen projectiles in atomic Mg, as a function of projectile energy. The total ε (labeled ''total''), the partial stopping cross sections of the two different charge states (labeled H^+ and H^0, respectively) considered in this work and the contribution due to charge exchange (labeled *c*-1) are shown.

of electrons by the projectile shields the long-range Coulomb interaction with the target electrons and the SCS decreases. In spite of its small cross section the contribution of electron capture to the SCS is still present at high energies, due to the large transition energy involved.

Figure 8 shows the theoretical SCS and the different contributions to it for hydrogen projectiles in solid Mg. The shape of the total SCS is again determined by the SCS of the bare ion fraction. However, by comparison with the gas phase, the curve is less peaked, with a smaller value at the maximum ($\varepsilon_{max}=18.9\times10^{-15}$ eV cm^2 at 70 keV) which is displaced towards higher energies. Two factors contribute to this behavior: the shape of the charge state distribution (see Fig. 6) and the smaller difference (in relative terms) between the SCS of protons and neutral hydrogen atoms in the solid phase. The screening of the proton by the Mg valence band electrons reduces the probability of exciting electrons in the medium.

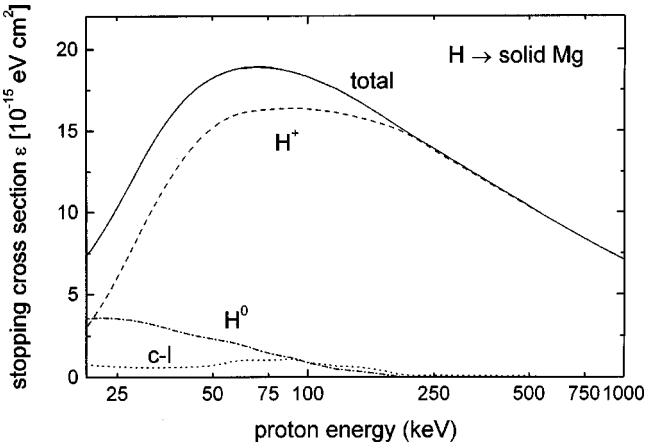

FIG. 8. Theoretical stopping cross section ε for hydrogen projectiles in solid Mg, as a function of projectile energy. The total ε (labeled ''total''), the partial stopping cross sections of the two different charge states (labeled H^+ and H^0, respectively) considered in this work and the contribution due to charge exchange (labeled *c*-1) are shown.

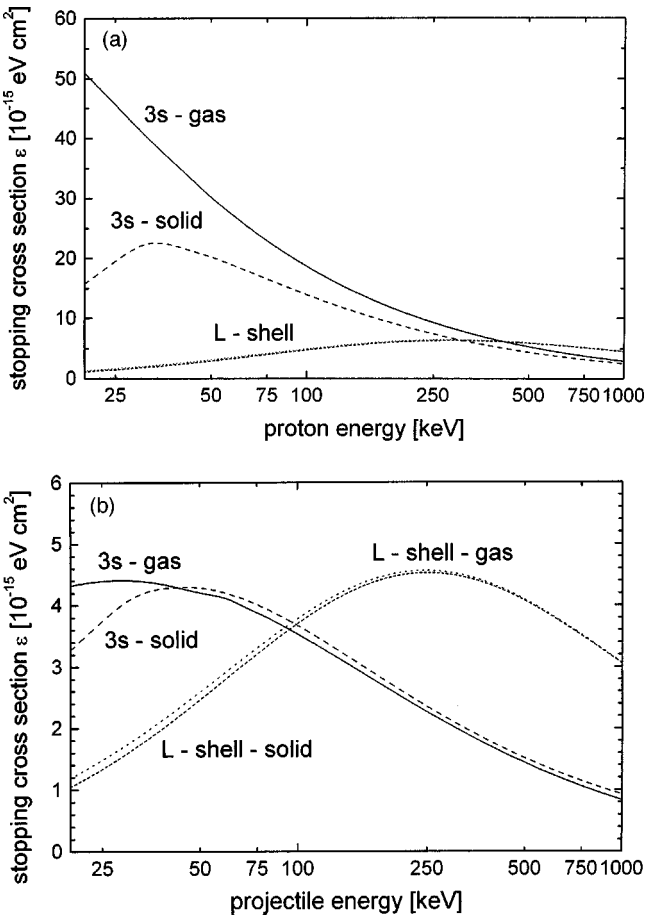

FIG. 9. Comparison between the theoretical stopping cross section ε of bare protons (a) and neutral hydrogen projectiles (b) in solid and gas Mg targets, as a function of the projectile energy (in keV). Two different mechanisms for the projectile energy loss are considered: excitation and ionization of the Mg 3*s* electrons, and excitation and ionizataion of the Mg *L*-shell electrons.

In Fig. 9 we plot the stopping cross sections for protons and neutrals in both phases. The contributions from *L* shell and *M* shell electrons are shown separately. The *L* shell contribution is essentially the same for the two phases, both for protons and hydrogen, except at very low energies where excitation and low-energy ionization play a role. However, the *M* shell contribution is quite different at low energies, especially for protons. It reflects the different range of interaction in the gas and in the metal, as well as the different screening. The measured phase effect is, however, smaller, since the fraction of protons decreases at low energies (see Fig. 6).

In Fig. 10 we present the theoretical SCS in the solid and in the gas phase together with the experimental data. Let us discuss theory first: the calculated SCS is larger in the gas phase, with a difference reaching a factor of two at low projectile energies. The phase effect is mainly due to the dynamic screening of the projectile (especially when it is a bare ion) by the Mg valence electrons in the solid phase. This is especially true when the dominant contribution to the total SCS is excitation and ionization of the Mg 3*s* electrons, as can be seen in Fig. 11, in which we plot the phase effect and the contribution to it coming from excitation and ionization of the Mg *M* shell. Figure 11 shows that the phase effect can

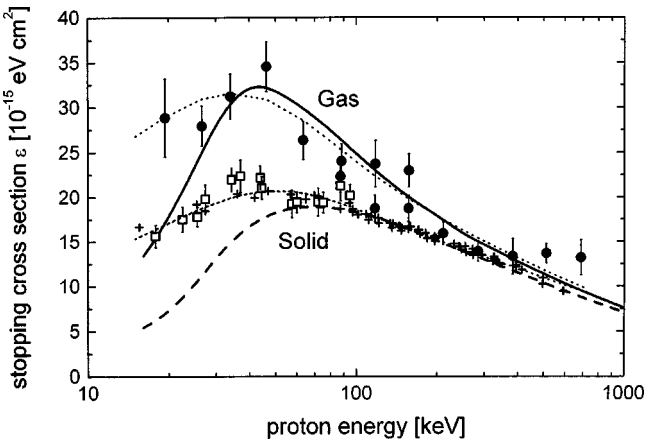

FIG. 10. Theoretical stopping cross section ε for hydrogen projectiles in solid Mg (long dashed line) and in Mg gas (solid line), as a function of proton energy, together with experimental data. Our present experimental data for the gas phase (full circles) are shown together with the data for the solid phase from Ref. 8 (open squares) and from Ref. 12 (+).

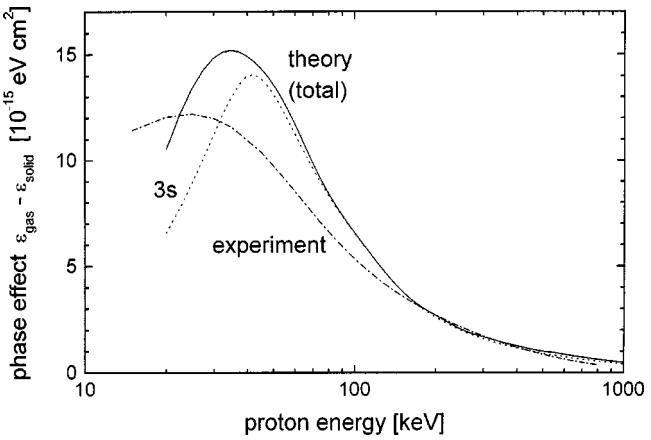

FIG. 11. Phase effect, $\varepsilon_{\mathrm{gas}}-\varepsilon_{\mathrm{solid}}$, for hydrogen projectiles in Mg as a function of the projectile energy. The experimental phase effect is represented by a dash-dotted line and the theoretical one by a solid curve. The contribution to the phase effect due to excitation processes of the Mg 3*s* electrons (dashed line) is also shown.

almost entirely be explained in terms of the difference in the Mg valence-electron contribution in the two phases. Additional contributions to the phase effect are caused by the difference in the charge states of the projectile in both phases and by the different transition energy involved in the capture and loss processes.

Let us now compare experiment and theory: In Fig. 10, we present the new data for the gas phase, and, for the solid, we show the data from Refs. 8 and 12. Comparing theory and experiment for the solid phase, we find excellent agreement in the energy range 70–600 keV. This indicates that the theoretical model is adequate, since the experimental data for the solid are absolute ones. For the gas phase, the agreement between theory and experiment is excellent over an even wider energy range, i.e., 30–680 keV. Since the normalization of the gas data at 400 keV was done by setting $\varepsilon_{\mathrm{gas}}^{(\mathrm{exp})}(390\,\mathrm{keV})-\varepsilon_{\mathrm{solid}}^{(\mathrm{exp})}(390\,\mathrm{keV})=\varepsilon_{\mathrm{gas}}^{(\mathrm{th})}(390\,\mathrm{keV})-\varepsilon_{\mathrm{solid}}^{(\mathrm{th})}(390\,\mathrm{keV})$ (see experimental part), the perfect agreement between experiment and theory for the solid phase also leads to agreement for the gas phase at this specific energy. The excellent agreement of measured and calculated gas data over such a wide energy range makes the normalization of the gas data trustable and it further supports the theoretical model. At very low energies (70 keV for the solid and 30 keV for the gas phase), the theory fails to describe properly the experimental data, due to the breakdown of the linear theory (first born approximation in calculating cross sections for the gas phase and dielectric response for the solid).

In Fig. 11, the experimental phase effect $\Delta\varepsilon$ compares favorably to the theoretical one, with excellent agreement for energies above 170 keV. Around 35 keV, theory overestimates the phase effect by about 25%, due to the fact that for the gas phase theory stays in accordance with experiment down to lower energies as compared to the solid phase.

At high energies the stopping cross sections in both phases converge to the same value. In this regime, inner-shell excitations also represent a significant part of the projectile energy loss and solid-state effects become less important in two respects: first because screening of the projectile by the target electrons is not so efficient, and second, because the energy loss depends on the number of target electrons rather than on their initial orbitals. The $1/E$ dependence of the phase effect $\Delta\varepsilon$ is expected to hold also at high energies (Bethe regime).

This experimental and theoretical study yielded detailed information on the phase effect in Mg and a thorough understanding of the underlying physical processes. On the basis of this knowledge, one can deduce information on any other system of interest, with a high level of accuracy.

ACKNOWLEDGMENTS

This work was partly supported by the Austrian Science Fund, under Project No. P9748-PHY, by Eusko Jaurlaritza, Euskal Herriko Unibertsitatea, Gipuzkoako Foru Aldundia, and the Spanish D.G.E.S. One of us (P.B.) expresses his gratitude for the kind hospitality in the group in San Sebastián.

*Also at Donostia International Physics Center, San Sebastián, Spain.

[1] J. R. Tesmer and M. Nastasi, *Handbook of Modern Ion Beam Materials Analysis* (Materials Research Society, Pittsburgh, 1995).

[2] P. M. Echenique, F. Flores, and R. H. Ritchie, in *Solid State Physics: Advances in Research and Applications*, edited by H. Ehrenreich (Academic, New York, 1990), Vol. 43, p. 229.

[3] K. Eder, D. Semrad, P. Bauer, R. Golser, P. Maier-Komor, F. Aumayr, M. Peñalba, A. Arnau, and P. M. Echenique, Phys. Rev. Lett. **79**, 4112 (1997).

[4] P. Bauer, F. Kastner, A. Arnau, A. Salin, P. D. Fainstein, V. H. Ponce, and P. M. Echenique, Phys. Rev. Lett. **69**, 1137 (1992).

[5] A. Arnau, P. Bauer, F. Kastner, A. Salin, V. H. Ponce, P. D. Fainstein, and P. M. Echenique, Phys. Rev. B **49**, 6470 (1994).

[6] F. Kastner, Ph.D. thesis, University of Linz, 1996.

[7] M. Bergsmann, Ph.D. thesis, University of Linz, 1998.
[8] M. Bergsmann, P. Hörlsberger, F. Kastner, and P. Bauer, Phys. Rev. B **58**, 5139 (1998).
[9] E. Lax, Taschenbuch für Chemiker und Physiker, Band I, 3rd ed. (Springer-Verlag, Berlin, 1967).
[10] G. Schrenk, diploma thesis, University of Linz, 1998.
[11] E. Steinbauer, A. Salin, A. Arnau, R. Diez-Muiño, F. Kastner, and P. Bauer, Nucl. Instrum. Methods Phys. Res. B **115**, 93 (1996).
[12] P. Fischer, Ch. Eppacher, G. Höfler, and D. Semrad, Nucl. Instrum. Methods Phys. Res. B **115**, 27 (1996).
[13] D. H. Madison, Phys. Rev. A **8**, 2449 (1973); E. J. McGuire, *ibid.* **26**, 1858 (1982); N. M. Kabachnik, Nucl. Instrum. Methods Phys. Res. B **69**, 76 (1992).
[14] M. R. C. McDowell and J. P. Coleman, *Introduction to the Theory of Ion-Atom Collisions* (North-Holland, Amsterdam, 1970).
[15] R. D. DuBois, Phys. Rev. A **32**, 3319 (1985).
[16] K. H. Berkner, R. V. Pyle, and J. W. Stearns, Phys. Rev. **178**, 248 (1969).
[17] K. G. Moses and A. H. Futch, Jr., Bull. Am. Phys. Soc. **11**, 344 (1966).
[18] I. M. Cheshire, Proc. Phys. Soc. London **84**, 89 (1964); Dz. Belkic, R. Gayet, and A. Salin, Phys. Rep. **56**, 279 (1979); Comput. Phys. Commun. **32**, 385 (1983).
[19] K. H. Berkner, I. Bornstein, R. V. Pyle, and J. W. Stearns, Phys. Rev. A **6**, 278 (1972).